Communications Research Centre Canada
An Agency of Industry Canada

Centre de recherches sur les communications Canada
Un organisme d'Industrie Canada

Measurement-based analysis of MIMO system performance in urban microcells

Report of Spectrum Research Project TWS-16

T.J. Willink

CRC Report No. CRC-RP-2005-002
Ottawa, Ontario

September 2005

IC

Canada

CRC

Communications Research Centre Canada
An Agency of Industry Canada

Centre de recherches sur les communications Canada
Un organisme d'Industrie Canada

Measurement-based analysis of MIMO system performance in urban microcells

Report of Spectrum Research Project TWS-16

T.J. Willink

CRC Report No. CRC-RP-2005-002
Ottawa, Ontario

September 2005

Canada

CRC

Measurement-based analysis of MIMO system performance in urban microcells

Report of Spectrum Research Project TWS-16

T.J. Willink

CRC Report No. CRC-RP-2005-002
Ottawa, September, 2005

Abstract

Systems employing multiple element antennas at the transmitter and receiver terminals in dense scattering environments such as urban microcells can provide an increase in the achievable spectral efficiency by exploiting the diversity in space and time. A great deal of effort to develop techniques, such as space-time coding and spatial multiplexing, which exploit this space-time diversity has been reported in the literature. However, most of this work has assumed an idealistic model for the channel which is rarely observed in practice. This report presents the results of analysis using channel measurements obtained in urban Ottawa, investigating the impact of antenna configuration on the performance of real systems. It is shown that such systems, commonly called multi-input multi-output (MIMO) systems, do indeed provide significant increases in spectral efficiency which can be exploited to improve performance and throughput. These increases do not, however, match those based on idealistic assumptions, with the result that system performance is quite significantly different than that predicted by theory.

Résumé

Les systèmes qui utilisent des antennes à él'ements multiples avec des terminaux de transmission et de réception dans des environnements de diffusion denses, comme des microcellules urbaines, peuvent augmenter le rendement spectral réalisable en exploitant la diversité spatio-temporelle. Selon la littérature, des efforts considérables ont été consacrés à l'élaboration de techniques tirant parti de la diversité spatio-temporelle, comme l'encodage spatio-temporel et le multiplexage spatial. Toutefois, la majorité de ces efforts s'appuyaient sur un modle idéaliste des canaux qui est rarement observé dans la pratique. Le présent rapport expose les résultats d'analyse des mesures de canal obtenues dans la région urbaine d'Ottawa lors d'une étude concernant l'incidence de la configuration des antennes sur le rendement de véritables systèmes. Selon ces résultats, de tels systèmes, connus sous le nom de « systèmes multientrées-multisorties » (MIMO), augmentent considérablement le rendement spectral qu'il est possible d'exploiter pour améliorer le rendement et le débit. Ces augmentations ne correspondent pourtant pas à celles fondées sur les hypothèses idéalistes, ce qui entraîne un écart important entre les rendements théorique et pratique des systèmes.

Executive Summary

Modern user applications will soon cause an unsupportable demand on the available spectrum. Many present systems are designed to exploit temporal diversity inherent in a multipath fading environment, such as an urban microcell or indoor picocell. It has long been known that additional diversity is available using the polarisation or spatial domains, but only in recent years has this potential been pursued with a significant amount of research activity. Systems exploiting diversity in the space and time (and polarisation) domains are called multi-input multi-output (MIMO) systems, referring to their multiple element antennas at the transmitter and receiver.

Most of the MIMO research reported in the literature addresses the characterisation and exploitation of 'idealistic' space-time channels, in which the spatial and temporal properties are modelled by tractable but unrealistic expressions. This has spawned an onslaught of papers proposing and evaluating signal processing techniques which appear to work well, but may contain features which prevent their practical application in real systems operating in real physical environments.

The objective of the work presented herein was to measure real MIMO channels in urban microcellular environments using the CRC MIMO testbed, and to investigate the performance of two classes of MIMO systems: space-time coding and spatial multiplexing. The impact of the antenna configuration was also of interest.

This project has demonstrated that MIMO systems operating in real environments are faced with channels whose spatial properties may diverge considerably from the theoretical. The impact is that system performance is not readily predicted using theoretical models, and furthermore, measurements obtained using single element antenna systems are not adequate to obtain the information required to assess real system performance.

In spite of this, it is clear that significant improvements in performance (error rates or throughput) are possible, confirming that MIMO technology does hold the key to increasing system capacity.

Sommaire Exécutif

Les applications des utilisateurs modernes imposeront bientôt une demande insoutenable sur le spectre disponible. De nombreux systèmes actuels sont conçus pour exploiter la diversit temporelle inhérente à un environnement d'évanouissement à trajets multiples, comme une microcellule urbaine ou une picocellule intérieure. On sait depuis longtemps que la polarisation ou les domaines spatiaux permettent d'utiliser la diversité additionnelle, mais ce potentiel ne fait l'objet de recherches importantes que depuis quelques années. Les systèmes qui exploitent la diversité des domaines spatial et temporel (et la polarisation) se nomment les ≪ systèmes multientrées-multisorties ≫ (MIMO), une dénomination qui fait référence aux antennes à éléments multiples des transmetteurs et des récepteurs.

La plupart des recherches sur les systèmes MIMO mentionnées dans la littérature s'attardent à la caractérisation et à l'exploitation des canaux spatio-temporels ≪ idéalistes ≫ dans lesquels les propriétés spatiales et temporelles sont représentées par des expressions solubles mais irréalistes. Cela a entrané la publication d'une quantité considérable d'articles proposant et évaluant des techniques de traitement des signaux qui semblaient efficaces, mais qui contenaient des caractéristiques rendant impossible l'application pratique de véritables systèmes dans des environnements physiques réels.

L'objectif des travaux présentés dans ce document consistait à mesurer de véritables canaux MIMO dans des environnements microcellulaires urbains à l'aide du banc d'essai MIMO du Centre de recherches sur les communications (CRC) et à analyser le rendement de deux catégories de systèmes MIMO, soit l'encodage spatio-temporel et le multiplexage spatial. L'incidence de la configuration des antennes était également à l'étude.

Ce projet a démontré que les systèmes MIMO fonctionnant dans des environnements réels devaient composer avec des canaux dont les propriétés spatiales pouvaient tre considérablement différentes des prévisions théoriques. Par conséquent, il n'est pas possible de prédire aisément le rendement des systèmes à l'aide de modèles théoriques, et les mesures obtenues au moyen de systèmes d'antennes à élément unique ne permettent pas d'obtenir les renseignements requis pour évaluer le véritable rendement des systèmes.

Malgré cela, il est possible d'améliorer considérablement le rendement (taux d'erreur ou débit), ce qui confirme que la technologie MIMO est le moyen permettant d'accrotre la capacité des systèmes.

Acknowledgements

This work was performed under the Industry Canada Spectrum Research program.

Thanks to Chris Squires, Geoff Colman and Jeff Wells (co-op student, Memorial University) for their excellent teamwork in undertaking the measurement campaign.

Contents

List of Figures

List of Tables

1 Introduction

Space-time systems exploit the diversity inherent in a multipath environment through the use of multi-element antennas (MEAs) at each end of the communications link. Such systems are commonly referred to as *multi-input multi-output* (MIMO) systems. The 'richness' of the scattering of the signal energy and the angular distribution of the scattering objects determine the potential gains available through space-time signal processing, Fig. 1. In much of the theoretical literature it is assumed that the scattering is 'rich', and space-time signal structures and detectors have been proposed and analysed for this channel. In more recent work, it has been acknowledged that most real channels do not have these ideal characteristics, and that achievable gains are likely to be lower than those promised by the theoretical approaches.

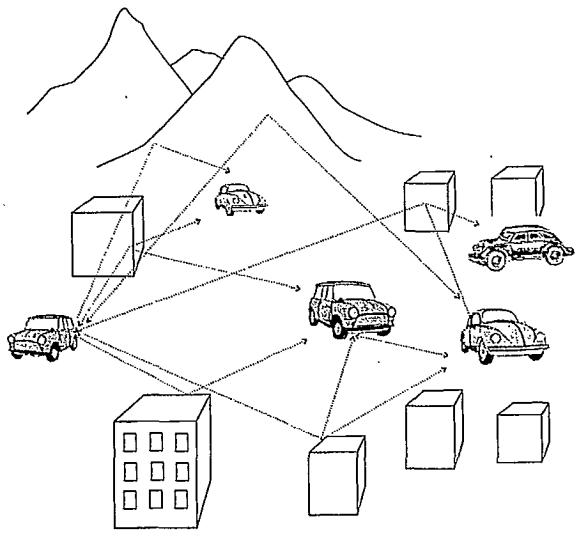

Figure 1. Multipath environment

As the demand for spectrum increases, to support more and more wireless users and high-rate, high QoS services, it is clear that significant increases in spectral efficiency are required. It is widely accepted that this can only be achieved through the use of MIMO technologies, therefore it is necessary to understand the capabilities of space-time channels to support high rate communications.

The objective of the work undertaken in this project was to determine realistic performance expectations for mobile terrestrial MIMO communications systems. The influence of antenna configuration was also a primary consideration, to determine the impact of the physical size and structure of the array.

The objective of the project has been achieved as follows. Measurements of MIMO channels were made in real operating environments, and the data collected were analysed to determine the channel characteristics such as maximum spectral efficiency and spatial correlation for different antenna element spacings at the transmitter and receiver. Space-time technologies typical of the two primary approaches to exploiting space-time diversity were simulated, and their performances were

evaluated using the real measured channel parameters and compared to that for 'ideal' channels.

1.1 System model

The narrowband multipath channel is modelled through the channel matrix, $\mathbf{H}$, in which the (i,j)th element, h_{ij}, represents the complex gain from transmitter element j to receiver element i, thus the received vector at the N_r-element array at time instant k is given by

$$\mathbf{r}(k) = \mathbf{H}(k)\mathbf{s}(k) + \mathbf{n}(k) \tag{1}$$

where $\mathbf{s}(k)$ is the length-N_t vector of transmitted symbols at instant k, and $\mathbf{n}(k)$ is the AWGN vector in which the elements are assumed to be i.i.d. with variance N_0.

In most of the available literature, the elements of $\mathbf{H}$ are assumed to be i.i.d. complex Gaussian random variables with zero mean and variance σ_h^2, denoted $\mathbf{H} \sim \mathcal{CN}\left(0, \sigma_h^2 \mathbf{I}\right)$. This assumption is based on having an infinite number of impinging wavefronts with equal average powers and uniformly distributed phase, arriving from angles distributed uniformly around the unit sphere. More recently, it is becoming recognised that the assumption of independence is not realised in most environments of interest, and that the elements of $\mathbf{H}$ are therefore correlated in some way. Various models have been proposed, but while in many cases they are mathematically tractable, they do not reliably reflect measured data.

Note that most technologies proposed thus far for MIMO communication systems are based on narrowband (frequency-nonselective) channels, and extension to wideband (frequency-selective) channels is achieved through the used of orthogonal frequency division multiplexing (OFDM).

1.2 Report organisation

In Sec. 2, the measurement equipment and data extraction are briefly described; more detail on this can be found elsewhere. The measurement campaign, including antenna configurations and routes, is also discussed in Sec. 2. The theoretical capacity of a MIMO channel and its relationship to correlation are reviewed in Sec. 3, followed by the evaluation of these quantities for the measured data. In Sec. 4, introductions to space-time coding and spatial multiplexing are provided, and results obtained for typical implementations of these concepts using the measured data are presented. Conclusions and recommendations are given in Sec. 5.

2 Measured MIMO channels

In order to assess the capabilities of real MIMO channels, measurements were taken in a microcell-type environment in urban Ottawa. The measurements were obtained using the CRC MIMO testbed, described briefly in Sec. 2.1, which was developed in the Radio Communications Technologies section primarily under the Defence Communications Program. The measurement campaign is described in Sec. 2.2.

2.1 CRC MIMO testbed

The CRC MIMO testbed provides the capability to measure real multi-dimensional channels in typical operating scenarios. As currently configured, the system supports eight transmitter antenna elements and eight receiver elements ('8 × 8' MIMO). The operating range is 20 MHz to 2.4 GHz with a bandwidth of up to 50 MHz; the system currently operates in an allocated 25 MHz bandwidth with centre frequency 2037.5 MHz.

For channel sounding, pseudo-noise (PN) sequences are transmitted from each transmitter element simultaneously. To maintain SNR and reduce the processing required to extract the channel impulse response estimates (CIREs), the PN sequences are (nearly) orthogonal. Blocks of data are recorded at each receiver element at a triggered rate of 250 Hz. These recorded data are then processed offline to obtain 64 CIREs, one for each transmitter-receiver pair. More details of the system and the post-processing are found in [1, 2].

For the purposes of the work in this project, only narrowband channels were of interest. Therefore, the CIREs were FFT'ed to provide the channel frequency response, and a single spectral line, corresponding to a frequency of 2.0383 GHz, was used to obtain the complex channel gains, $h_{ij}(k)$, which are the elements of the channel matrix $\mathbf{H}(k)$.

2.2 Channel measurements

For the channel characterisations described herein, the antenna elements were arranged in uniform linear arrays, with a spacing of one-half wavelength, $\lambda/2$. The transmitter was placed in the corner window of the fourth floor in the Minto Place Suites Hotel, at 45° to the direction of Slater St. The receiver was installed in the measurement van, with the array mounted on the roof at a height of approximately 2 m. The mobile unit was driven along the routes shown in Fig. 2.

To determine the impact of antenna configurations, the measured data were processed as 4 × 4 MIMO channels with inter-element spacings of $\lambda/2$ and λ. The resulting configurations are described by the spacing of the transmitter and receiver elements as:

$$(1/2\lambda, 1/2\lambda) \quad (1/2\lambda, 1\lambda) \quad (1\lambda, 1/2\lambda) \quad (1\lambda, 1\lambda).$$

It is clear from Fig. 2 that the power levels received will vary along the measurement route due to shadowing and path loss. To assess the effect of the local multipath fading only, a simple power control was applied by normalising the measured channel matrix such that $\mathcal{E}\left\{\|\mathbf{H}(k)\|_F^2\right\} = \sum_{i,j} \mathcal{E}\left\{|h_{ij}(k)|^2\right\} = N_r \cdot N_t$ over discrete time intervals of 200 ms.

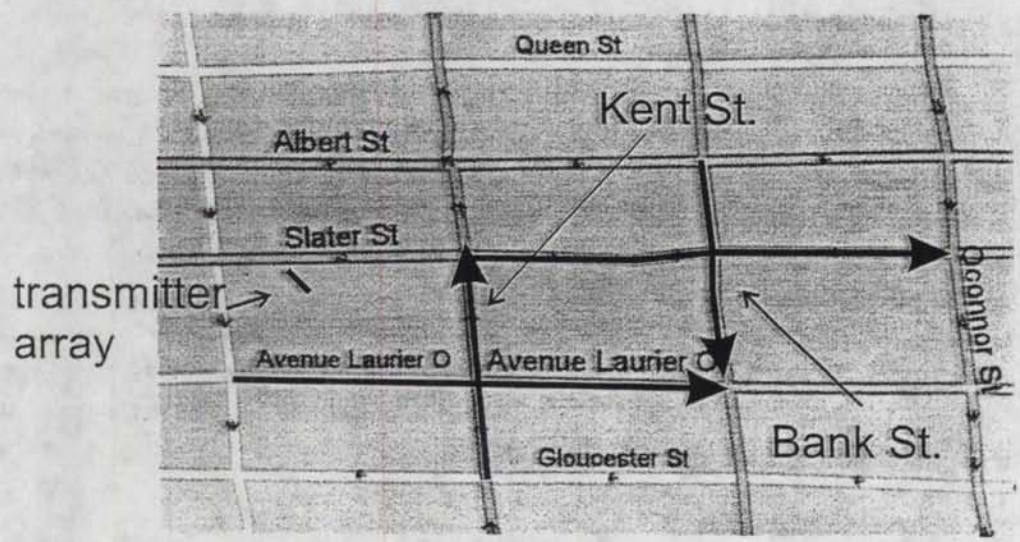

Figure 2. Location of transmitter and routes of receiver in urban Ottawa.

3 Channel characteristics

The routes were chosen to give a variety of channel conditions. The 'ideal' i.i.d. complex Gaussian model is based on an isotropic assumption, i.e., the signals are assumed to arrive with equal average powers and uniformly distributed phases from directions uniformly distributed around the receiver. One important feature that affects the potential for improved spectral efficiency is the angular distribution of the received signals, Sec. 3.1.

The most common metric of the channel's capability to support communications is the *capacity*, measured in bits/s, or *spectral efficiency* (capacity per unit bandwidth, bits/s/Hz). As will be seen in Sec. 3.2, the capacity of a channel is closely related to the autocorrelation of the channel matrix. Thus, the maximum available spectral efficiency and the channel correlation statistics have been extracted from the measured data and are presented in Sec. 3.3 and Sec. 3.4, respectively.

3.1 Angles of arrival

The distribution of the angles of arrival of the multipath components affects the diversity available in the MIMO channel, and hence its potential for increasing system performance. If the element spacing is small, a narrow angular spread typically leads to a high correlation and correspondingly low capacity.

There are many methods of estimating angles of arrival; for high accuracy, super-resolution techniques such as MUSIC, ESPRIT, SAGE, etc. are often used but these require a high computational complexity. A more practical technique is the Capon minimum variance method, as follows. For a series of channel responses, $\mathbf{H}(k)$, for which the structure of multipath components is consistent, the sampled autocorrelation matrix

$$\mathbf{R} = \frac{1}{K} \sum_{k=k_0+1}^{k_0+K} \mathbf{H}(k)\mathbf{H}^H(k) \tag{2}$$

is generated. For steering vectors

$$\mathbf{a}(\theta) = \frac{1}{\sqrt{N_r}} \left[1 \quad e^{-j\beta d\cos(\theta)} \quad \cdots \quad e^{-j\beta(N_r-1)d\cos(\theta)} \right]^T \tag{3}$$

where θ is the angle to array broadside, $\beta = 2\pi/\lambda$ and d is the inter-element spacing, the power at a given angle, $P(\theta)$, is calculated using

$$P(\theta) = \frac{1}{\mathbf{a}^H(\theta)\mathbf{R}^{-1}\mathbf{a}(\theta)}. \tag{4}$$

Fig. 3 shows the received angular power over the measurement routes, estimated using (4). The autocorrelation matrix was generated using $K = 20$ consecutive measurements of $\mathbf{H}$ and the angular power was calculated every 160 ms along the routes. Along Slater St., there are dominant angular components at approximately $\pm 10°$ which change very little in the corridor between Kent St. and Bank St., and similarly for a short distance along the corridor beyond Bank St.; these dominant specular components correspond to single reflections from each side of the street. On

Laurier Ave. the signals arrive predominantly from one side, with angles in the range 30° to 70°. Along Bank St. the signals arrive almost equally from both sides. This is consistent with the non-line-of-sight conditions, with signals predominantly arriving after reflection from buildings on both sides of the street. On the Kent St. route, in the first few seconds there is a dominant signal whose angle changes from approximately 150° to 90°. The cause of this is not clear at this point. Further along the route, there is a dominant, consistent component from one side, with other angular multipath components being received over a wide range of angles. Recall that a simple power control algorithm has been applied to the measurements, therefore the impact of path loss and strong local variations has largely been removed.

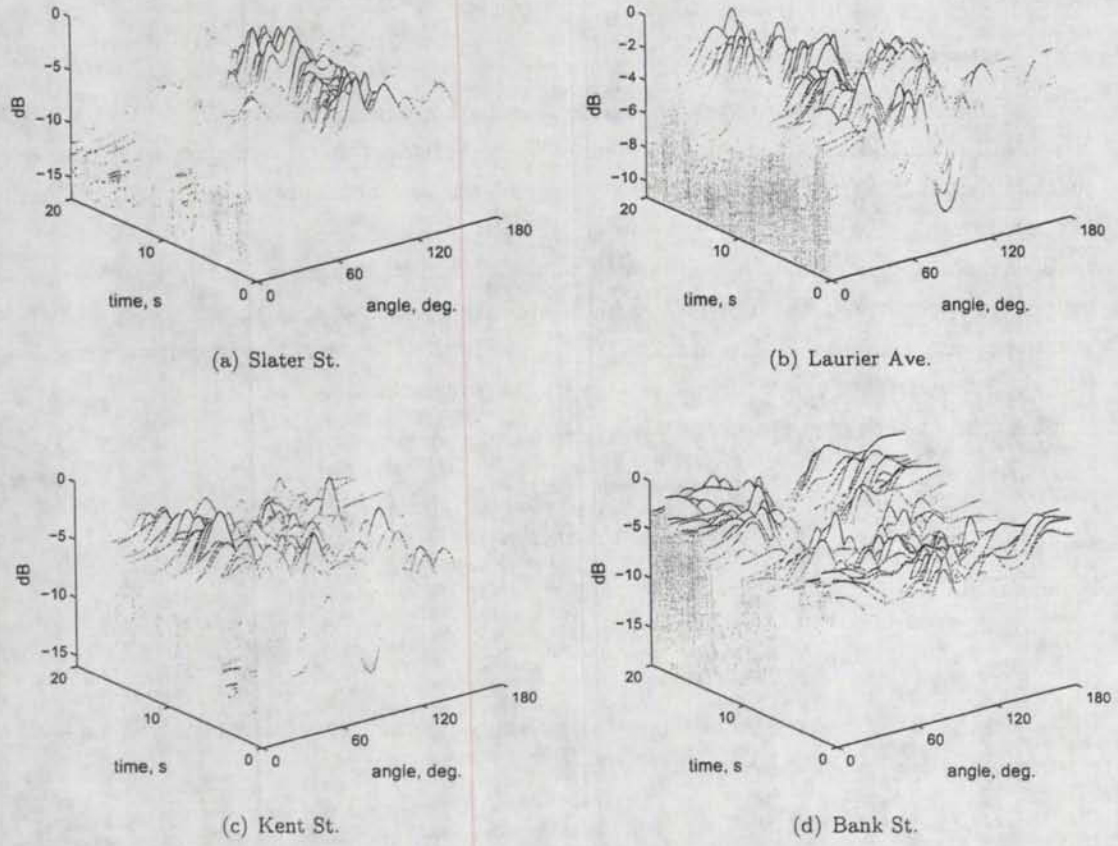

(a) Slater St.

(b) Laurier Ave.

(c) Kent St.

(d) Bank St.

Figure 3. Angles of arrival.

3.2 Capacity

The channel capacity is a theoretical concept, and is the maximum average amount of information that can be transmitted over the channel, generally measured in bits/s. It should be noted that the

achievable throughput will be less than the capacity, but it is the objective of the signal processing, in conjunction with error correction coding, to approach it. The capacity is a function of bandwidth, therefore for channel measurements, the more useful metric is spectral efficiency, given by capacity per unit bandwidth, in bits/s/Hz.

3.2.1 SISO channels

For a single-input, single-output (SISO) additive white Gaussian noise (AWGN) channel, it can be shown [3, Ch. 8] that the capacity for a channel of bandwidth W with uniform spectral response h is given by

$$C = W \log\left(1 + \frac{P|h|^2}{N_0 W}\right) \tag{5}$$

where the two-sided noise power spectral density is $N_0/2$, the total transmit power is P. (Note that, when the units of C are bits/s, the log function is base-2.)

When the channel response of a frequency-selective channel is known at the transmitter, (5) leads to the well-known 'water-filling' solution, in which the bandwidth is divided into N parallel channels of bandwidth W_i with gains $|h_i|^2$, and the capacity is then

$$C = \sum_{i=1}^{N} W_i \log\left(\frac{|h_i|^2 \mu}{N_0 W_i}\right) \tag{6}$$

where the power allocated to each parallel channel is given by

$$p_i = \left(\mu - \frac{N_0 W_i}{|h_i|^2}\right)^+ \tag{7}$$

and $(a)^+ = \max(a, 0)$, such that $\sum_i p_i = P$. Thus μ is the waterfill level, such that $\mu = p_i + N_0 W_i/|h_i|^2$. The data transmitted on channel i to achieve this theoretical solution is Gaussian distributed, at rate

$$C_i = W_i \log\left(\frac{|h_i|^2 \mu}{N_0 W_i}\right). \tag{8}$$

When the channel state information is not available at the transmitter, the solution for maximum capacity is to transmit equal data rates with equal power over each of the N subchannels, then

$$C = \sum_{i=1}^{N} W_i \left(1 + \frac{P}{N N_0 W_i}|h_i|^2\right). \tag{9}$$

Another useful concept is the *outage capacity*, C_{out}, which is the level below which C falls for some defined percentage of the time, i.e., the 5% outage capacity is the level which will be achieved 95% of the time, i.e.,

$$P_{out} = Pr(C < C_{out}) = 0.05. \tag{10}$$

3.2.2 MIMO channels

When the channel matrix $\mathbf{H}$ is known at the transmitter, the transmitted signal substreams may be preprocessed, i.e., the transmitted signal becomes

$$\mathrm{x}(k) = \mathbf{X}\mathbf{P}^{\frac{1}{2}}\mathrm{s}(k) \tag{11}$$

where $\mathbf{X}$ describes the spatial mapping of the elements of $\mathrm{s}(k)$ and $\mathbf{P} = diag(p_1, \cdots, p_{N_t})$ is the power allocation matrix. In this case, the capacity of the narrowband MIMO ('space-selective') channel is given, in a parallel way to the SISO frequency-selective case, by [4]

$$C = \max_{\mathbf{Q}} W \log\det\left(\mathbf{I} + \frac{P}{N_0 W}\mathbf{H}\mathbf{Q}\mathbf{H}^H\right) \tag{12}$$

where $\mathbf{Q} = \mathcal{E}\left\{\mathrm{x}(k)\mathrm{x}^H(k)\right\}$ is the input covariance matrix and $\mathrm{tr}(\mathbf{Q}) = 1$. The capacity is maximised when $\mathbf{Q}$ is selected such that the channel matrix $\mathbf{H}$ is divided into orthogonal spatial subchannels, equivalent to the frequency subchannels in the frequency-selective SISO case. This is achieved when the eigenmodes of $\mathbf{H}$ are used for transmission, in which case the number of modes that can be supported depends on the eigenvalues λ_i, which are equivalent to the gains $|h_i|^2$ in the SISO case.

The MIMO capacity for channel state information at the transmitter is then

$$C = \sum_{i=1}^{\min(N_t, N_r)} W \log\left(\frac{\mu\lambda_i}{N_0 W}\right). \tag{13}$$

where the power allocated to subchannel i is

$$p_i = Q_{ii}P = \left(\mu - \frac{N_0 W_i}{\lambda_i}\right)^+ \tag{14}$$

where Q_{ii} is the ith diagonal element of $\mathbf{Q}$ and μ is again the waterfill level, this time in the space dimension, such that $\mu = p_i + N_0 W_i/\lambda_i$.

In general, the transmitter does not have channel state information, then it can be shown that, when the elements of $\mathbf{H}$ are i.i.d. complex Gaussian, the optimum transmit strategy is to divide the transmitter power equally among the transmitting antenna elements, i.e., (11) becomes $\mathrm{x}(k) = \mathrm{s}(k)$. The capacity is then given by

$$C = W \log\det\left(\mathbf{I} + \frac{P}{N_t N_0 W}\mathbf{H}\mathbf{H}^H\right) \tag{15}$$

which can be written in terms of the eigenvalues of $\mathbf{H}\mathbf{H}^H$ as

$$C = \sum_{i=1}^{\min(N_t, N_r)} W \log\left(1 + \frac{P}{N_t N_0 W}\lambda_i\right). \tag{16}$$

The relationship between the gains of the orthogonal spatial subchannels, i.e., the eigenvalues λ_i, in the 'space-selective' (MIMO) case, (16), and the orthogonal frequency subchannels, $|h_i|^2$, in the

frequency-selective (SISO) case, (9), is again clear. Note that the concept of *outage capacity* also applies here.

Thus the channel capacity is determined by the distribution of the eigenvalues of the channel autocovariance matrix, which are determined by the spatial correlation of the transmitter-receiver pair links.

3.3 Measured spectral efficiency

The maximum achievable spectral efficiency was calculated using (16) for the measured data along all four routes, using each of the four antenna configurations. The cumulative distribution functions (CDFs) of the results at an average received SNR of 20 dB are shown in Fig. 4. The spectral efficiencies of the 'ideal', i.e., i.i.d. complex Gaussian, case are also shown for SISO (1×1) and MIMO (2×2 and 4×4) with markers '$\times$'.

First, note that on all channels, there is a significant gain in spectral efficiency available through the use of MIMO systems on the measured routes, which are typical of an urban microcell. Additionally, note that the available spectral efficiency increases when the element spacing at the transmitter and receiver is increased from $\lambda/2$ to λ on all routes, although the relative gain is not the same in all cases. On Slater St. and Bank St. a larger gain is observed due to increased spacing at the receiver, whereas on Laurier Ave. and Slater St. the gain is larger when the spacing at the transmitter is increased. The available spectral efficiency is lowest on the Slater St. route, which is consistent with the observation of a strong specular component in Fig. 3. On Laurier Ave., the available spectral efficiency is very close to the theoretical maximum for all configurations. The corresponding outage spectral efficiencies are shown in Table 1 for $P_{out} = 0.05$; the outage spectral efficiency for the 'ideal' i.i.d. complex Gaussian channel model is approximately 19 bits/s/Hz. Note that these results are quite different if power control is not applied.

Table 1. Outage spectral efficiencies for an outage probability of $P_{out} = 0.05$.

Route	Outage spectral efficiency, bits/s/Hz			
	$(1/2\lambda, 1/2\lambda)$	$(1\lambda, 1\lambda)$	$(1/2\lambda, 1\lambda)$	$(1\lambda, 1/2\lambda)$
Slater St.	14.3	15.5	15.5	14.3
Laurier Ave.	17.4	17.8	17.6	17.8
Kent St.	16.2	18.0	16.5	17.3
Bank St.	13.6	16.3	15.7	14.0

3.4 Measured correlation statistics

As noted above, the capacity of a MIMO channel is related to the correlation through the eigenvalues of the channel's autocorrelation matrix. To assess the degree of correlation at the receiver terminal, the normalised autocorrelation matrix $\mathbf{R}_r$ was formed for each route. Recall that h_{ij}, the (i,j)th element of $\mathbf{H}$, represents the complex gain from transmitter element j to receiver element i, then

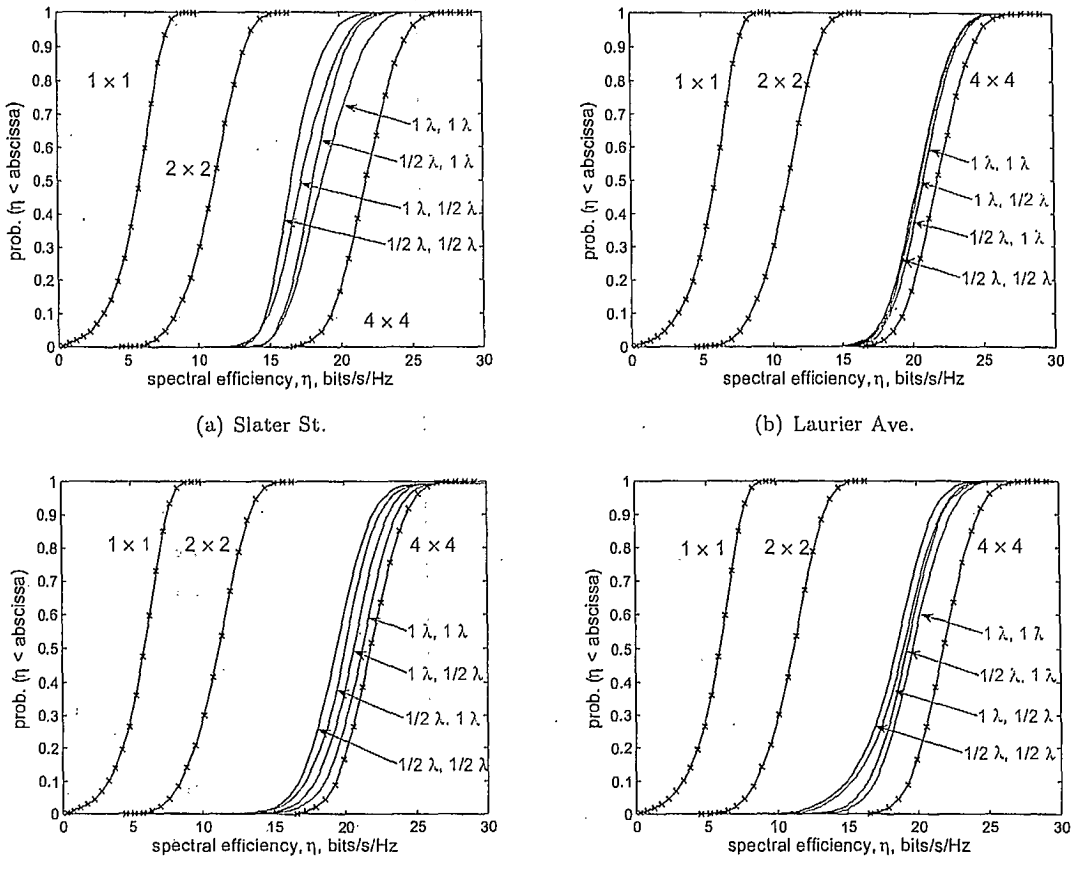

(a) Slater St. (b) Laurier Ave.

(c) Kent St. (d) Bank St.

Figure 4. CDFs of maximum achievable spectral efficiency.

the elements of $\mathbf{R}_r$ are

$$[\mathbf{R}_r]_{ij} = \frac{\frac{1}{K}\sum_{k=1}^{K}\sum_{t=1}^{N_t} h_{ti}^{*} h_{tj}}{\left[\left(\frac{1}{K}\sum_{k=1}^{K}\sum_{t=1}^{N_t}|h_{ti}|^2\right)\left(\frac{1}{K}\sum_{k=1}^{K}\sum_{t=1}^{N_t}|h_{tj}|^2\right)\right]^{\frac{1}{2}}} \tag{17}$$

i.e., the correlation coefficients between the complex vector responses at the receiver array to signals from transmitter elements i and j. The normalisation ensures the diagonal elements of $\mathbf{R}_r$ are unity.

To evaluate the degree of spatial correlation at the transmitter, the autocorrelation matrix $\mathbf{R}_t$

was generated, for which the (i,j)th element is specified by

$$[\mathbf{R}_t]_{ij} = \frac{\frac{1}{K}\sum_{k=1}^{K}\sum_{t=1}^{N_t} h_{it}^* h_{jt}}{\left[\left(\frac{1}{K}\sum_{k=1}^{K}\sum_{t=1}^{N_t}|h_{it}|^2\right)\left(\frac{1}{K}\sum_{k=1}^{K}\sum_{t=1}^{N_t}|h_{jt}|^2\right)\right]^{\frac{1}{2}}} \tag{18}$$

i.e., the correlation coefficients between the complex vector responses at the transmitter array for signals arriving at receiver elements i and j. (Alternatively, $[\mathbf{R}_t]_{ij}$ represents the correlation between the array responses that would occur at the transmitter array for signals transmitted from elements i and j of the receiver array.)

It was seen in [5, 6] that the channel parameters are consistent over distances of 2 m to 6 m, and are therefore likely to be wide-sense stationary. Therefore, the expectations in (17) were taken over $K = 45$ data points, corresponding to a distance of approximately 2 m at 40 km/hr. The CDFs of the off-diagonal ($[\mathbf{R}_r]_{ij}$ for $i \neq j$) elements in (17) are shown in Fig. 5, and the equivalents for $\mathbf{R}_t$ are shown in Fig 6. The receiver and transmitter correlations measured along Slater St. are very high, consistent with the angular power distribution observed in Sec. 3.1 and with the observations of available spectral efficiency noted in Sec. 3.3. For the Laurier Ave. measurement, the plots show a lower degree of correlation than the i.i.d. complex Gaussian case; this seems contradictory, as the i.i.d. CG case is, by definition, uncorrelated. However, this situation could arise when the number of angular multipath components is quite small, as supported by the observations in Sec. 3.1. Note that while the correlation distributions are similar at the transmitter and receiver terminals on most routes, along Bank St. the spatial correlation is markedly higher at the transmitter than at the receiver. This is indicative of the signals from the transmitter being 'tunnelled' along Slater St., thus having a small angular spread (high correlation), and then diffracted into Bank St. and arriving at the receiver array with a wide angular spread, i.e., low correlation, as observed in Sec. 3.1. It is somewhat surprising that this is not observed also along Kent St., but this may be due to the more 'open' corner at Slater St. and Kent St., versus the higher building density at the corner of Slater St. and Bank St.

The results confirm that, in general, the spatial correlations are lower when the element spacing is larger, as expected.

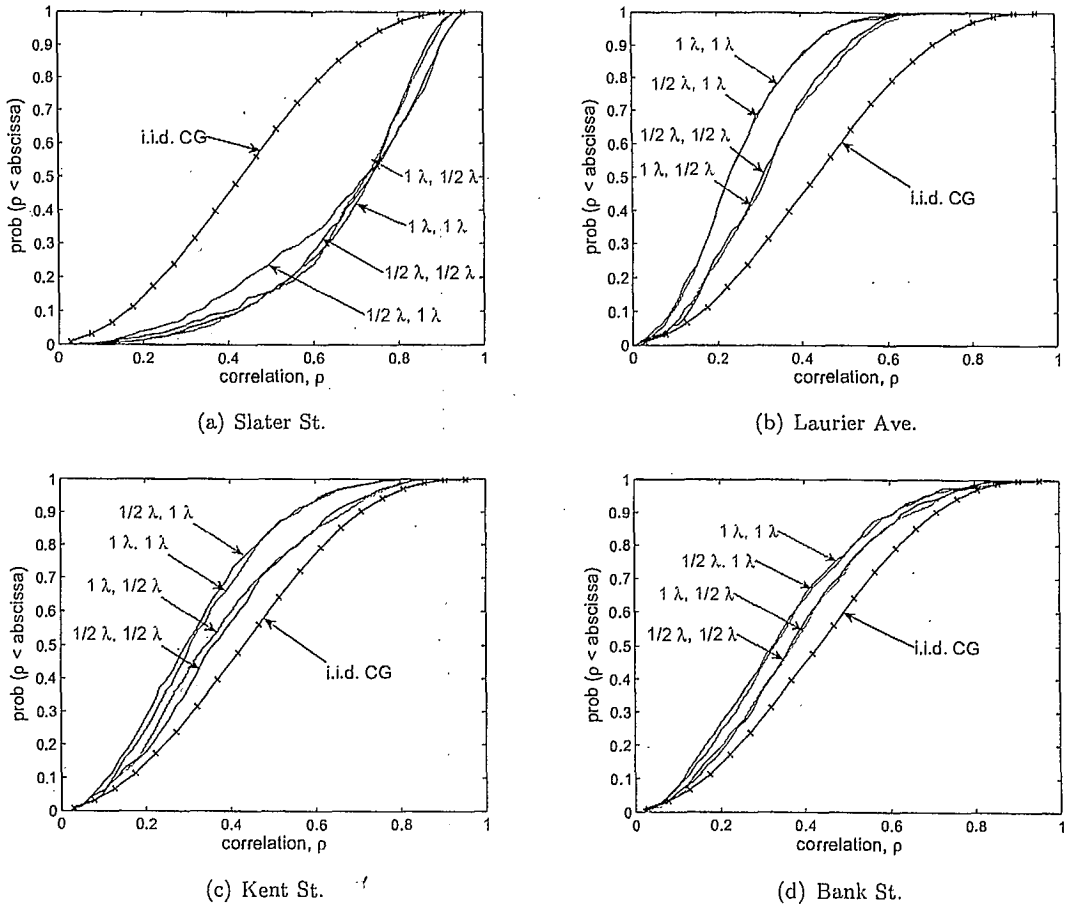

(a) Slater St.

(b) Laurier Ave.

(c) Kent St.

(d) Bank St.

Figure 5. CDFs of receiver array response correlation coefficients.

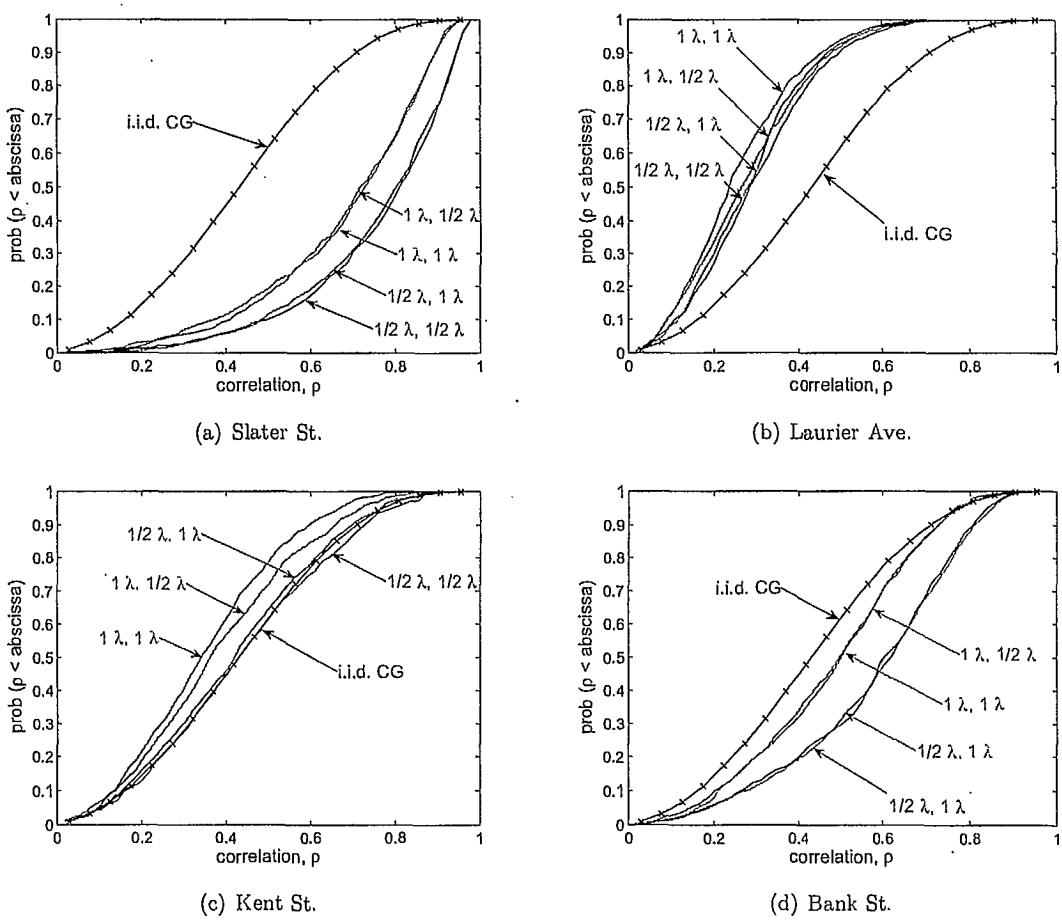

(a) Slater St.

(b) Laurier Ave.

(c) Kent St.

(d) Bank St.

Figure 6. CDFs of transmitter array response correlation coefficients.

4 Expected performance of MIMO systems

In Sec. 3, the maximum available spectral efficiencies and spatial correlations were found for the measured data. It was clear that the characteristics of the real channels do not fit the theoretical models for which most signalling techniques have been developed, i.e., the i.i.d. complex Gaussian channel. Therefore, it is important to evaluate the performance of typical MIMO signalling techniques on real channels to determine realistic performance expectations.

In Sec. 4.1, an overview of space-time coding is given, and the performance of a specific code is determined using simulations based on the measured data. Spatial multiplexing is discussed in Sec. 4.2, and simulations are again used to demonstrate the expected performance over the measured channels.

4.1 Space-time coding

In most wireless systems, the dominant effect on performance is fading. The effects of fading can be mitigated using space-time coding, which exploits the spatial and temporal diversity of the channel. It is used when the link between each transmitter element and the receiver, with an array or a single element antenna, is not robust enough to provide the desired performance. The technique introduces redundancy by transmitting the information multiple times over the space-time domain. In general, space-time coding improves bit error performance but may not increase the data rate.

Space-time codes, which take the form of block or trellis codes, are designed for a specific number of transmitter elements, and can be received using single or multiple element antennas. For trellis codes, introduced in [7], the number of states in the trellis increases exponentially as the number of transmitter elements increases. Additionally, while increasing the array size improves performance by increasing diversity, the incremental diversity gain decreases as N_t becomes large. Thus, space-time trellis codes are practical and useful only for a small number of transmitter antenna elements.

Unlike trellis codes, in which the impact of a single information symbol has an extended effect on the trellis state, the temporal signature of space-time block codes (STBCs) is limited to the length of the code. This allows for a lower complexity decoder. Many STBC designed do not provide a coding gain, but achieve performance improvement through diversity gain. A commonly-used example is the 2×2 Alamouti block code [8]. With this code, two data symbols (s_1 and s_2) are transmitted over two symbol periods, i.e., for a single receiver element,

$$\begin{bmatrix} r_1 & r_2 \end{bmatrix} = \begin{bmatrix} h_1 & h_2 \end{bmatrix} \begin{bmatrix} s_1 & -s_2^* \\ s_2 & s_1^* \end{bmatrix} + \begin{bmatrix} n_1 & n_2 \end{bmatrix} \tag{19}$$

where r_1 and r_2 are the symbols received in the first and second time intervals, respectively, and n_1 and n_2 are the corresponding noise components. The symbols are simply decoded using

$$\begin{bmatrix} \hat{s}_1 \\ \hat{s}_2 \end{bmatrix} = \begin{bmatrix} h_1^* & h_2 \\ -h_2^* & h_1 \end{bmatrix} \begin{bmatrix} r_1 \\ r_2 \end{bmatrix}. \tag{20}$$

While this is a simple and attractive (and patented) technique, it was noted in [9] that there are no full-rate complex codes of this type for more than $N_t = 2$ transmit antenna elements, and no full-rate real codes for $N_t > 8$.

For the results used in this section, a four-dimensional *quasi-orthogonal* STBC was used; instead of achieving a diversity gain of $4N_r$, the gain is $2N_r$. When all $N_r = 4$ are used, the loss in diversity gain is relatively small. The code is defined as [10]

$$A = \begin{bmatrix} s_1 & -s_2^* & -s_3^* & s_4 \\ s_2 & s_1^* & -s_4^* & -s_3^* \\ s_3 & -s_4^* & s_1^* & -s_2 \\ s_4 & s_3^* & s_2^* & s_1 \end{bmatrix}. \tag{21}$$

Note that each symbol, s_i, $i = 1, \ldots, 4$ is transmitted once during each time interval, and once from each transmitter element. This ensures that each symbol has the same reliability in detection. This code is detected using a maximum-likelihood (ML) technique, as described in [10].

4.1.1 Performance

The 4-dimensional quasi-orthogonal code was implemented for QPSK modulation and evaluated for channel matrices given by the measured data described in Sec. 2. CDFs of the bit error rate (BER) results using $N_r = 4$ receiver elements are shown in Fig. 7 at 6 dB for each of the four routes. As discussed above, STBCs are intended also for use when there are fewer receiver than transmitter elements; results are shown in Fig. 8 for a single receiver element at 9 dB. In these results, it is assumed that the receiver has perfect channel knowledge. In the real case, in which estimation errors degrade the channel state information, the impact will be similar to increased receiver noise, i.e., lower SNR.

The trends of the STBC performance with $N_r = 4$ do not follow those of the spectral efficiency CDFs in Sec. 3.3. The BER achieved on Slater St. and Bank St. is lower than on Laurier Ave., and that on Kent St. is significantly higher than the other three. This is contrary to the spectral efficiency evaluation, which indicated higher spectral efficiencies available on Kent St. and Laurier Ave. Furthermore, the order of performance for the four antenna element configurations on Slater St. is not the same as the spectral efficiency order.

However, note from Fig. 5 and Fig. 6 that the highest correlation at the transmitter and receiver is observed on the Slater St. measurement. This correlation results in constructive combining of the received signals more often than destructive, leading to a higher average SNR. Furthermore, the specular component of the signal provides a stable contribution to the received signals, reducing the effects of the multipath fading component. This also explains why, in Fig. 8, the performance using $1/2\lambda$ transmitter element separation is better than for the 1λ separation; it was seen in Sec. 3.4 that this case has the highest spatial correlation at the transmitter. The performance on Laurier Ave. and Bank St. with $N_r = 1$ is quite similar, this is consistent with the relatively small difference observed in their transmitter correlations. The anomaly is the performance on Kent St.; it is not explained by the transmitter correlations which fall between those of Laurier Ave. and Bank St.

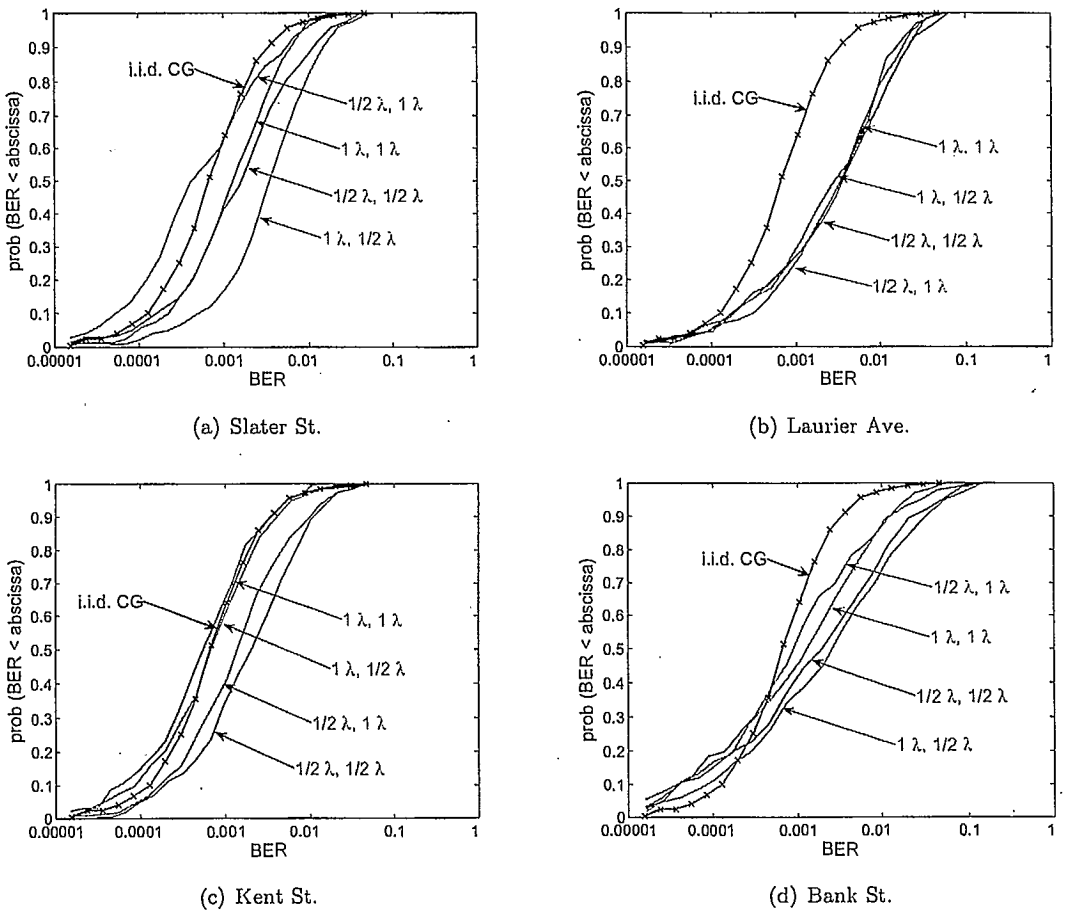

(a) Slater St.

(b) Laurier Ave.

(c) Kent St.

(d) Bank St.

Figure 7. CDFs of performance of quasi-orthogonal STBC with QPSK at 6 dB, with $N_r = 4$.

Fig. 9 shows the CDFs of BER for $N_r = 4$ on Kent St. using the $(1/2\lambda, 1/2\lambda)$ array configurations for different SNRs. It is seen that the BER cannot be fully recovered by increasing the SNR; the channel characteristics cause a higher proportion of high BER situations than would be expected on an ideal channel even as the SNR is increased.

4.2 Spatial multiplexing

Spatial multiplexing is used to achieve an increase in throughput over MIMO channels, but may result in a decrease in performance. It is used if the response for a single data substream, e.g., from an individual transmitter element to the receiver array, is robust; generally, there must be at least as many elements in the receiver array as at the transmitter, i.e., $N_r \geq N_t$.

The description of capacity suggests that an effective approach to MIMO signalling would be to direct the signal power along the eigenmodes, with suitable power allocation, to mimic the capacity solution. This technique is called *eigen-beamforming*. The channel matrix H has singular value

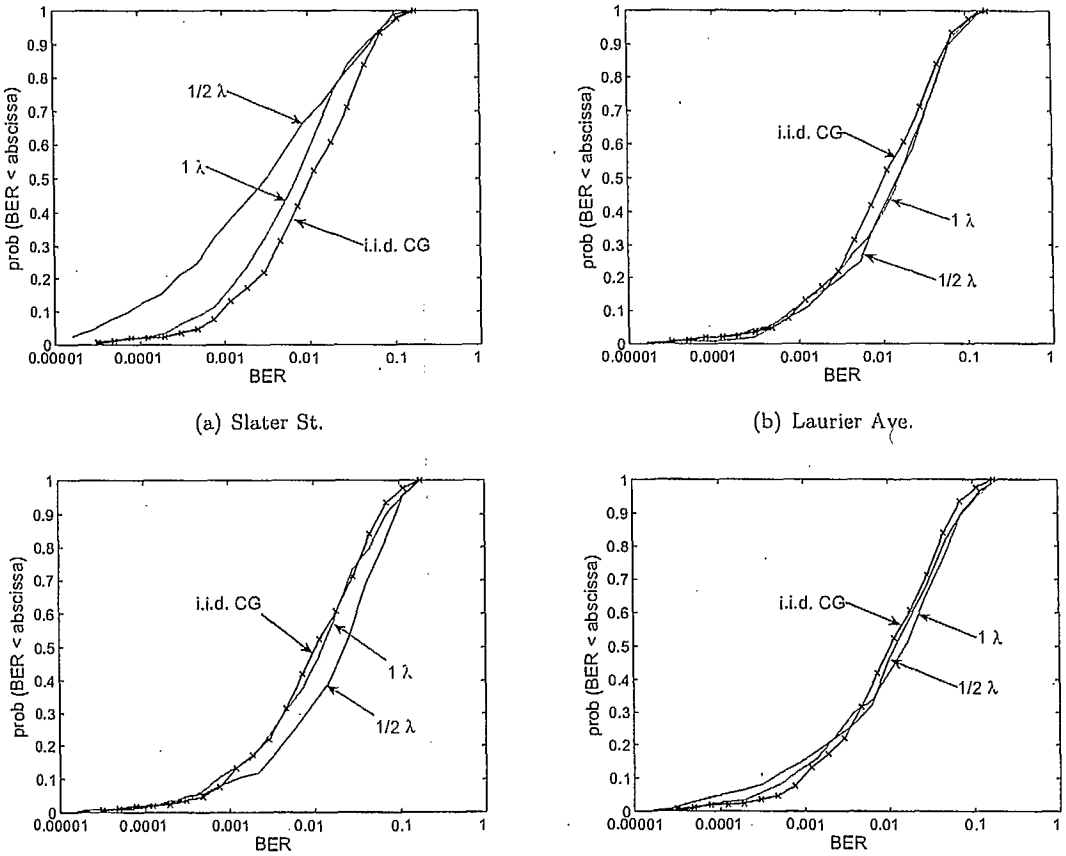

(a) Slater St.

(b) Laurier Ave.

(c) Kent St.

(d) Bank St.

Figure 8. CDFs of performance of quasi-orthogonal STBC with QPSK at 9 dB, with $N_r = 1$.

decomposition

$$\mathbf{H} = \mathbf{U}\tilde{\Sigma}\mathbf{V}^H \tag{22}$$

where the columns of the $N_r \times N_r$ and $N_t \times N_t$ unitary matrices $\mathbf{U}$ and $\mathbf{V}$ are the left and right singular vectors of $\mathbf{H}$, respectively, and

$$\tilde{\Sigma} = \begin{cases} \begin{bmatrix} \Sigma & 0 \end{bmatrix} & N_r < N_t \\ \begin{bmatrix} \Sigma \end{bmatrix} & N_r = N_t \\ \begin{bmatrix} \Sigma & 0 \end{bmatrix}^T & N_r > N_t \end{cases} \tag{23}$$

and the $N = \min(N_t, N_r)$ non-zero entries in the diagonal matrix $\Sigma = diag(\sigma_1, \sigma_2, \ldots, \sigma_N)$ are the singular values of $\mathbf{H}$. For eigen-beamforming, the transmitter performs a linear precoding of the form $\mathbf{X} = \mathbf{V}$ in (11). At the receiver, the signal substreams are detected using

$$\hat{\mathbf{s}}(k) = \mathbf{U}^H \mathbf{r}(k) \tag{24}$$

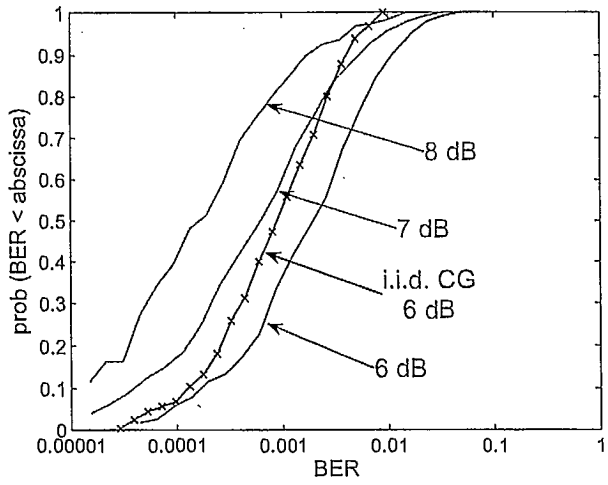

Figure 9. CDFs of quasi-orthogonal STBC performance on Kent St. using $(1/2\lambda, 1/2\lambda)$ with $N_r = 4$.

which results in

$$\hat{s}_i(k) = \sigma_i \sqrt{p_i}\, s_i + \nu_i \quad i = 1, \ldots, N \tag{25}$$

where ν_i is the AWGN on the ith eigenmode.

This technique, which relies on accurate channel state information at the transmitter, was proposed in [11] for a fixed wireless access system in which the terminals were located high above the traffic and the fading rate was minimal, thus the channel changed little during the feedback interval. In mobile environments, in which the channel changes quite rapidly and there is a limited number of noisy samples from which to estimate $\mathbf{H}(k)$, the inaccuracies in channel estimation lead to self-interference which can significantly degrade the system performance [12]. This is therefore not a feasible approach to achieving improved spectral efficiencies in highly mobile environments, despite its inclusion in some wireless standards.

Another approach, not requiring channel state information at the transmitter, is to transmit parallel independent data substreams simultaneously from each of the transmitter elements with equal power. Linear spatial processing is generally unable to provide enough interference reduction to enable detection with sufficient accuracy, unless $N_r \gg N_t$. Nonlinear spatial processing was proposed in [13, 14]; it is called V-BLAST, for vertical Bell-Labs space-time architecture. This is based on a simple, but computationally complex, successive interference cancellation (SIC) approach, in which the strongest signal is detected first using linear spatial processing, then its contribution to the received signal vector is cancelled. The second strongest signal is then detected in a similar way. Thus, error propagation is minimised, but not eliminated, by detecting the strongest signal at each step, i.e., that which is least likely to be in error.

4.2.1 Performance

The V-BLAST detector was evaluated for channel matrices given by the measured data described in Sec. 2 for QPSK modulation. CDFs of the bit error rate (BER) results are shown in Fig. 10 for each of the four routes, with a SNR of 12 dB.

The trend of the results follows the CDFs of spectral efficiency, i.e., a higher theoretical spectral efficiency generally results in a lower BER. However, note that there does not appear to be a linear relationship between the V-BLAST performance and spectral efficiency.

Note that, as in Sec. 4.1.1, these results were obtained assuming perfect channel state information at the receiver. With channel estimation errors the performance degrades, especially for correlated channels, as the estimation errors result in irreducible self-interference.

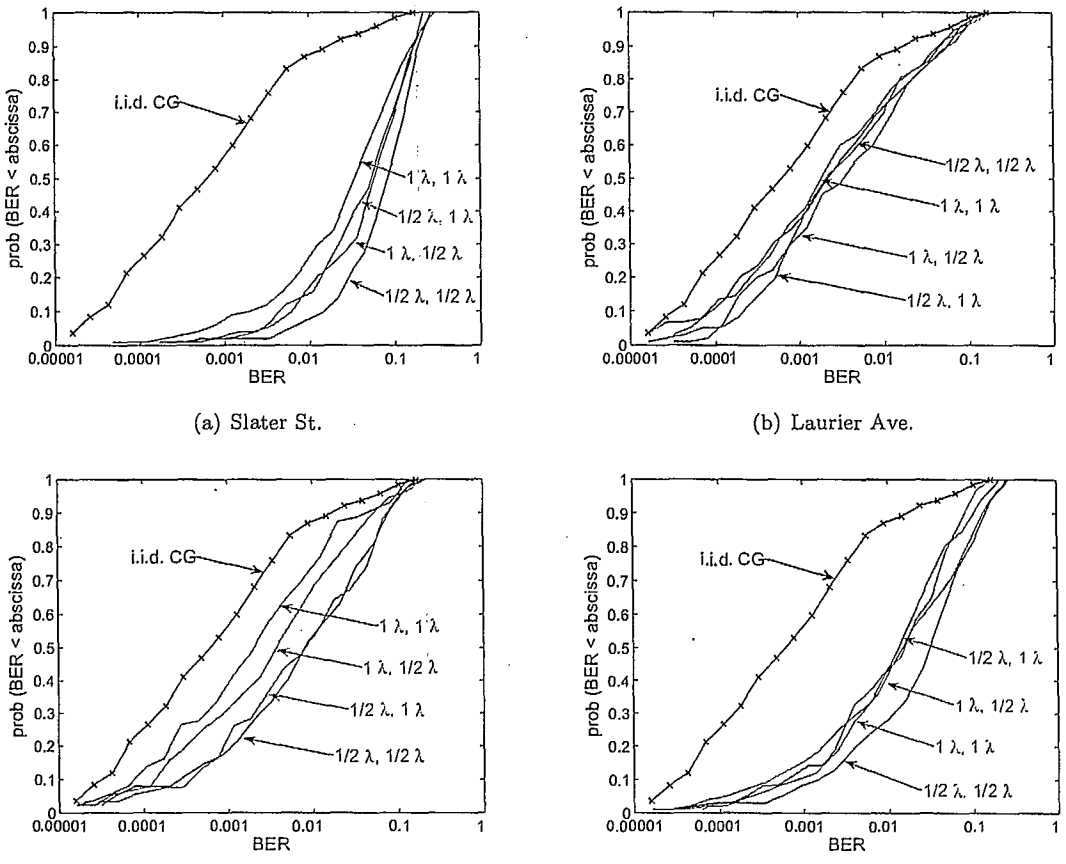

(a) Slater St.

(b) Laurier Ave.

(c) Kent St.

(d) Bank St.

Figure 10. CDFs of performance of spatial-multiplexing with V-BLAST using QPSK at 12 dB.

Fig. 11 shows the CDFs of BER on Kent St. using the $(1/2\lambda, 1/2\lambda)$ array configurations for different SNRs. It is seen that the BER can be recovered by increasing the SNR. This is consistent with the observation above that the spectral efficiency and BER are related – at fairly high SNRs,

the spectral efficiency increases almost linearly with SNR.

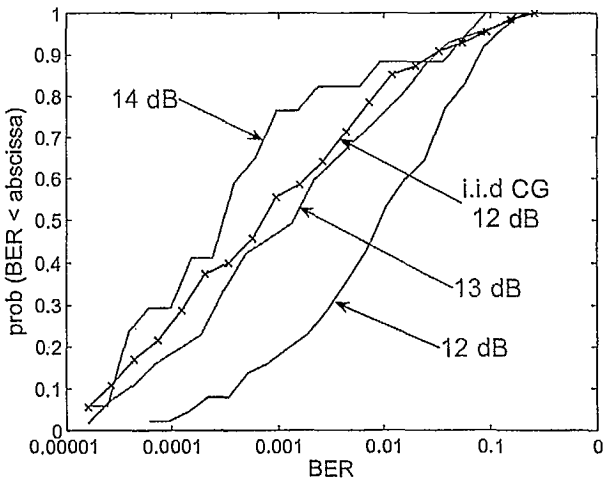

Figure 11. CDFs of V-BLAST performance on Kent St. using $(1/2\lambda, 1/2\lambda)$.

5 Conclusions

It has been demonstrated that substantial increases in spectral efficiency are possible using MIMO systems, which employ multiple element antennas at the transmitter and receiver. These systems exploit the space-time diversity inherent in a multipath environment to improve system performance using space-time coding or to increase throughput using spatial multiplexing.

Measurements in a typical urban microcell have shown that the spectral efficiencies achievable using MIMO systems in real environments are lower than those expected using 'ideal' theoretical models, but are nonetheless significantly higher than those provided by SISO systems.

The antenna element spacing has some impact on the measured spectral efficiency; as expected, inter-element spacing of one wavelength is better than using one-half wavelength. However, the relative impact of spacing at the transmitter and receiver is highly dependent on the specific location, and it is not true to say that the spacing at one terminal is always more significant than that at the other.

The performance of MIMO transmission and signal processing techniques is clearly linked to the observed channel characteristics, but there is not a straightforward relationship. Channel characteristics such as number, power and relative delays of angular multipath components, angular spread and fading distributions impact the eigenvalue distribution of the channel's autocorrelation matrix, and thereby the spectral efficiency, in a different way than they impact the performance of space-time coding and multiplexing techniques.

It was observed during the analysis that the normalisation of the channel measurements, equivalent to power control, is significant when considering the distributions of the spectral efficiencies and system performances. Furthermore, for some but not all MIMO techniques in some environments, increasing power may regain the performance lost due to non-ideal channel characteristics. A detailed investigation of the impact of power control in MIMO systems is beyond the scope of this project.

Clearly, MIMO will be a critical part of future mobile wireless communication systems, as the demand for services increases. The reliability of such systems is highly dependent on the specific environment in which they operate. There is insufficient information available from single element antenna measurements to determine realistic performance parameters, and current theoretical analyses do not represent the variability of MIMO channels within a local environment with sufficient accuracy to be useful in system planning. Therefore, in implementing such systems, it will be necessary to measure the environments specifically using multiple element antenna systems.

While the theoretical analysis of MIMO systems suggests a spatial multiplexing approach using the eigenmodes of the channel matrix (eigenbeamforming), a consideration of realistic effects such as channel estimation errors indicates that such systems have limited practical applicability. Even though eigenbeamforming may be incorporated into some wireless standards, its effectiveness in mobile environments is limited.

References

[1] T. Willink, B. Gagnon, Y. De Jong, and R. Bultitude, "A MIMO measurement and demonstration system for advanced space-time signalling techniques," in *Proc. ANTEM 2002*, (Montreal, QC), July 2002.

[2] C. Squires, T. Willink, and B. Gagnon, "A flexible platform for MIMO channel characterisation and system evaluation," in *Proc. WIRELESS 2003 - Proc. 15th Int. Conf. on Wireless Commun.*, (Calgary, AB), July 2003.

[3] R. Gallager, *Information Theory and Reliable Communication*. New York: Wiley & Sons, 1968.

[4] E. Telatar, "Capacity of multi-antenna Gaussian channels," *Euro. Trans. Telecommun.*, vol. 10, pp. 585–595, Nov.-Dec. 1999.

[5] R. Bultitude, G. Brussaard, M. Herben, and T. Willink, "Radio channel modelling for terrestrial vehicular mobile applications," in *Proc. ICAP/JINA Millennium Conference on Antennas and Propagation*, (Davos, Switzerland), Apr. 2000.

[6] R. Bultitude, T. Willink, M. Herben, and G. Brussaard, "Detection of changes in the spectral characteristics of measured mobile radio data for space wave modelling applications," in *Proc. Queen's University Bienniel Symposium on Communications*, (Kingston, Canada), pp. 90–94, May 2000.

[7] V. Tarokh, N. Sheshadri, and A. Calderbank, "Space-time codes for high data rate wireless communication: performance criterion and code construction," *IEEE Trans. Inform. Theory*, vol. 44, pp. 744–765, Mar. 1998.

[8] S. Alamouti, "A simple transmit diversity technique for wireless communications," *IEEE J. Select. Areas Commun.*, vol. 10, pp. 1451–1458, Oct. 1998.

[9] V. Tarokh, H. Jafarkhani, and A. Calderbank, "Space-time block codes from orthogonal designs," *IEEE Trans. Inform. Theory*, vol. 45, pp. 1456–1467, July 1999.

[10] H. Jafarkhani, "A quasi-orthogonal space-time block code," *IEEE Trans. Commun.*, vol. 49, pp. 1–4, Jan. 2001.

[11] T. Willink, "MIMO OFDM for broadband fixed wireless access," *IEE Proc. Commun.*, vol. 152, pp. 75–81, Feb. 2005.

[12] T. Willink, "Improving power allocation to MIMO eigenbeams under imperfect channel estimation," *IEEE Commun. Lett.*, vol. 9, pp. 622–624, July 2005.

[13] P. Wolniansky, G. Foschini, G. Golden, and R. Valenzuela, "V-BLAST: an architecture for realizing very high data rates over the rich-scattering wireless channel," in *1998 URSI Int. Symp. on Signals, Systems, and Electronics, 1998*, pp. 295–300, Sept. 1998.

[14] G. Golden, G. Foschini, R. Valenzuela, and P. Wolniansky, "Detection algorithm and initial laboratory results using V-BLAST space-time communication architecture," *Elect. Lett.*, vol. 35, Jan. 1999.